HHS Public Access

Author manuscript

Macromol Biosci. Author manuscript; available in PMC 2016 September 01.

Published in final edited form as:

Macromol Biosci. 2015 September ; 15(9): 1218–1223. doi:10.1002/mabi.201500178.

Synergistic Effects of SDF-1α and BMP-2 Delivery from Proteolytically Degradable Hyaluronic Acid Hydrogels for Bone Repair

Dr. Julianne L. Holloway,
Department of Bioengineering, University of Pennsylvania, 210 S 33rd St, Philadelphia PA, 19104, USA

Henry Ma,
Department of Bioengineering, University of Pennsylvania, 210 S 33rd St, Philadelphia PA, 19104, USA

Reena Rai,
Department of Bioengineering, University of Pennsylvania, 210 S 33rd St, Philadelphia PA, 19104, USA

Prof. Kurt D. Hankenson, and
Department of Physiology, Michigan State University, 567 Wilson Rd, East Lansing MI, 48824, USA

Prof. Jason A. Burdick*
Department of Bioengineering, University of Pennsylvania, 210 S 33rd St, Philadelphia PA, 19104, USA

Summary

In order to achieve adequate bone repair, bone morphogenetic protein-2 (BMP-2) is typically delivered in large, non-physiological doses and can result in significant adverse side effects.[1] To reduce the amount of BMP-2 necessary for bone formation, we delivered another molecule, stromal cell derived factor-1α (SDF-1α), which is involved in stem cell recruitment[2,3] in combination with BMP-2. An engineered hyaluronic acid (HA) hydrogel that degrades via matrix metalloproteinases (MMPs) was used to deliver both molecules and release was mediated by protease level. A critical-sized calvarial defect model was used to assess biomolecule delivery on bone formation. The treatment group with combined SDF-1α and BMP-2 hydrogel delivery showed significantly higher bone formation when compared to hydrogels loaded with the same BMP-2 or SDF-1α concentration alone and was comparable to BMP-2 at an order of magnitude higher concentration, suggesting that the combined delivery of both biomolecules synergistically improves osteogenesis.

*burdick2@seas.upenn.edu.

Supporting Information

Supporting Information is available from the Wiley Online Library or from the author.

Keywords

hydrogel; hyaluronic acid; bone tissue engineering; bone morphogenetic protein; stromal cell-derived factor-1α

Introduction

Approximately 1.6 million bone grafts are performed in the United States every year;[4] however, significant drawbacks exist to this approach, including a limited tissue supply and donor site morbidity.[5] As an alternative to grafts, growth factor delivery is a common approach to induce bone formation.[6] Recombinant human BMP-2 and BMP-7, delivered using resorbable collagen sponges, are FDA-approved for use in spinal fusions and long bone non-union defects;[7,8] however, these procedures are costly, require supraphysiological doses (as high as 12 mg per collagen scaffold)[9], and release profiles are not optimal.[10]

Stromal cell-derived factor-1 (SDF-1) is upregulated after injury and is important for stem cell homing in both normal and injured tissues through the CXC chemokine receptor type 4 (CXCR4).[2,3,11] CXCR4 has been identified on hematopoietic and non-hematopoietic cell types, including mesenchymal stem cells (MSCs).[12] SDF-1 binds to CXCR4 and results in cellular migration in the direction of an SDF-1 gradient.[3] Kitaori et al. observed that SDF-1 is upregulated during the repair of a murine femoral bone graft and that new bone formation is inhibited with an anti-SDF-1 neutralizing antibody.[2] Blocking the SDF-1/CXCR4 axis of MSCs in vitro inhibited BMP-induced alkaline phosphatase activity, bone nodule formation, and Runx2 expression.[13] Recombinant SDF-1 has been delivered alone or in combination with BMP-2 via adsorption onto an electrospun fibrous scaffold[14] or collagen sponge[15] to improve bone repair.

To build on this work and introduce an engineered hydrogel for controlled delivery, we investigated the sustained delivery of both SDF-1α and BMP-2 from MMP-degradable HA hydrogels for bone repair. Hydrogels engineered for MMP-sensitivity can mimic the native remodeling mechanism of the extracellular matrix (ECM) and dynamically release growth factors in response to local proteases[16-18] and HA is a naturally occurring polysaccharide found throughout the body and is known to contribute to wound healing, ECM production, and osteogenesis.[19-21] We previously showed that HA is capable of inducing cell chemotaxis via the CD44 receptor[22] and that MMP-degradable HA-based hydrogels can deliver BMP-2 to bone defects.[18]

Hydrogels were formed by combining maleimide-modified HA (MaHA) with a monofunctional cell-adhesive peptide and a bifunctional MMP-sensitive peptide, where the thiols within the cysteine residues on the peptides allowed for rapid crosslinking via an addition reaction with the maleimide functional groups (**Figure 1a**). All hydrogels were synthesized to yield a final polymer concentration of 2 wt% using MaHA with a 30% maleimide functionalization of HA repeat units, and a bulk hydrogel concentration of 2 mM RGD. Hydrogel mass loss and biomolecule release as a function of time and collagenase concentration are shown in **Figure 1b-d**. In general, biomolecule release from MaHA

hydrogels was controlled as a function of collagenase concentration with little to no initial burst release. Minimal hydrogel mass loss was observed over the course of the study (~30%) for all hydrogels placed in buffer without collagenase; however, complete hydrogel degradation occurred rapidly and within 9 and 4 days for hydrogels in 1 and 2 U/mL collagenase, respectively. The approximate linear trend in hydrogel degradation suggests surface erosion as opposed to bulk degradation, potentially due to the small hydrogel mesh size, typically less than 100 nm,[23] when compared to collagenase size (~80 kDa).

Biomolecule release closely matched hydrogel degradation, with limited release (less than 50%) in the absence of collagenase and more rapid release with increasing collagenase concentration due to higher availability of MMPs to degrade the hydrogel crosslinks. This suggests biomolecule release occurs primarily through hydrogel degradation as opposed to through diffusion out of the hydrogel. Despite the relatively small size of SDF-1α (MW ~8 kDa), release was sustained, potentially through interactions with BMP-2 or the hydrogel. In vitro SDF-1α bioactivity was confirmed using a three-dimensional cell pellet invasion assay, where there was limited cell invasion from the pellet into the hydrogel material without SDF-1α and cell invasion was observed in the presence of SDF-1α (**Figure 1S**).

A critical-sized rat calvarial defect model was used to assess the efficacy of MaHA hydrogels for therapeutic release.[24] To investigate the effect of combined delivery of SDF-1α and BMP-2 on BMP-induced osteogenesis, a very low dose of BMP-2 (0.1 μg BMP-2) was selected, which does not typically initiate bone repair. Combined biomolecule delivery was compared to each biomolecule delivered alone, as well as a higher dose of BMP-2 (1.0 μg BMP-2) known to be adequate for significant new bone formation using this animal model.[18] The hydrogel formulation remained the same as in the release studies. Typical radiographs for all six groups are shown in **Figure 2a** and quantification of percent radiopacity is shown in **Figure 2b**. Statistically significant increases in radiopacity were observed for hydrogels loaded with 1.0 μg BMP-2 and with both 0.1 μg BMP-2 and 1.0 μg SDF-1α compared to the empty defect ($p < 0.05$).

To further evaluate new bone formation, μCT was used to quantitatively measure bone volume within each calvarial defect (**Figure 2c, 2d** and **Figure 2S)**. Both bone volume and defect score showed similar trends compared to the observed trends in radiopacity, where similar statistically significant increases were observed for hydrogels loaded with 1.0 μg BMP-2 and with both 0.1 μg BMP-2 and 1.0 μg SDF-1α compared to the empty defect ($p < 0.05$). For all metrics (radiopacity, bone volume, defect score), no other hydrogel treatment group showed significant differences compared to the empty defect ($p > 0.05$). Interestingly, for hydrogels loaded with both 0.1 μg BMP-2 and 1.0 μg SDF-1α, all reconstructed images indicated bone bridging across the widest part of the defect (score = 4). No other treatment group showed a similar level of bone bridging. When either SDF-1α or the low dose of BMP-2 was delivered separately, no significant bone repair was observed compared to the empty defect, suggesting a synergistic effect when SDF-1α and BMP-2 are delivered together. Also, closer evaluation of the μCT cross-sections (Figure 2c) shows a majority of new bone formation around the periphery of the hydrogel for the hydrogel loaded with 1.0 μg BMP-2 and more within the original defect area for the hydrogel loaded with both 0.1 μg

BMP-2 and 1.0 μg SDF-1α suggesting the delivery of SDF-1α contributes to cell invasion into the hydrogel material.

Histology was used to evaluate tissue morphology and cellular invasion into MaHA hydrogels after six weeks *in vivo* (**Figure 3)**. For the empty defect, minimal new bone formation was observed and the defect was filled with a thin fibrous layer. For the other treatment groups, the hydrogel material stained a light purple. In general, minimal new bone formation was observed histologically, except for the treatment groups where the hydrogels were loaded with 1.0 μg BMP-2 or both 0.1 μg BMP-2 and 1.0 μg SDF-1α. Additionally, higher magnification of the boundary between the hydrogel and bone tissue shows increased cell invasion into hydrogels loaded with SDF-1α. Increased cell invasion into the hydrogels was expected, as SDF-1α is known for recruiting stem cells to injury sites to promote tissue regeneration.[2,3,13]

In summary, a proteolytically degradable HA hydrogel system was used to deliver BMP-2 in combination with SDF-1α for improved bone repair. Biomolecule release from HA hydrogels was controlled through hydrogel degradation in the presence of collagenase, where limited release occurred through diffusion from the hydrogel. In vivo bone formation indicated that combined biomolecule release of both SDF-1α and BMP-2 is capable of synergistically improving new bone formation and resulted in a magnitude decrease in the effective BMP-2 dose for osteogenesis. Additionally, SDF-1α delivery resulted in improved cell invasion into the hydrogel material.

Experimental Section

Maleimide-functionalized hyaluronic acid (MaHA) synthesis

Maleimide-functionalized hyaluronic acid (MaHA) was synthesized according to a two-step protocol as described previously.[18,25,26] Briefly, the tetrabutylammonium salt of HA (HA-TBA) was synthesized from sodium hyaluronate (90 kDa, Lifecore Biomedical) and reacted with aminoethylmaleimidetrifluoroacetate salt (MA; Sigma-Aldrich) and benzotriazole-1-yl-oxytris-(dimethylamino)-phosphonium hexafluorophosphate (BOP; Sigma-Aldrich) in anhydrous dimethyl sulfoxide (DMSO; Fisher) to form MaHA, which was then frozen, lyophilized, and analyzed with ^{1}H NMR to determine functionalization.

MaHA hydrogel formation

Hydrogels were formed by first combining 30% functionalized MaHA dissolved in phosphate buffered saline (PBS; Gibco) and the cell-adhesive peptide GCGYG*RGD*SPG (RGD; Mw: 1025.1 Da; italics indicate cell-adhesive domain) for 30 minutes at 4°C to form the hydrogel precursor solution.[25] Gel formation was then initiated by adding the bifunctional MMP-sensitive peptide GCRDVPMS↓MRGGDRCG (Mw: 1696.96 Da; down arrow indicates MMP cleavage site) to the hydrogel precursor solution. Both peptides were obtained from GenScript (Piscataway, NJ). All hydrogels were synthesized by reaction at room temperature for 30 minutes to yield a final concentration of 2 wt% MaHA and 2 mM RGD, with a theoretical equimolar ratio between cysteines and maleimide groups.

Hydrogel degradation and biomolecule release

MaHA hydrogels were loaded with 100 ng BMP-2, 100 ng SDF-1α, or 100 ng of both SDF-1α and BMP-2 (R&D Systems) and compared to unloaded hydrogels. Hydrogels were formed using cylindrical acrylic molds with a volume of 40 μL (n=4). Hydrogels were placed in 1 mL Triton-Tris-Calcium buffer (TTC; 0.05 (v/v)% Triton X 100 (Sigma-Aldrich), 50 mM tris hydrochloride (EMD Biosciences), 1mM calcium chloride (Sigma-Aldrich), pH 7.4) with 2, 1, or 0 U/ml collagenase type II (CLS 2, Worthington Biochemical Corporation) at 37°C. The solution was changed every 24 hours until complete degradation or the study was terminated and the collected hydrogel degradation solutions were stored at −20°C until analysis. After the final time point, any remaining samples were degraded in 1 mg/ml hyaluronidase (Sigma-Aldrich). The amount of uronic acid, a degradation component of HA, within the hydrogel degradation solutions was quantified using a modified uronic acid assay.[27] SDF-1α and BMP-2 were quantified using an enzyme-linked immunosorbent assay (ELISA) kit (R&D Systems).

In vivo calvarial defect

A critical-sized 8 mm defect was created using a trephine in the crania of Sprague Dawley rats (250–275 g, male, Charles River) that were anesthetized using isoflurane. The craniotomy segment was removed and the defect was filled with the hydrogel material or left empty to serve as a negative control (n=3 per sample group for a total of 18 animals). Five hydrogel treatment groups were investigated: (1) MaHA hydrogel alone, (2) MaHA hydrogel with 1.0 μg BMP-2, (3) MaHA hydrogel with 0.1 μg BMP-2, (4) MaHA hydrogel with 1.0 μg SDF-1α, and (5) MaHA hydrogel with 1.0 μg SDF-1α and 0.1 μg BMP-2. The hydrogel precursor solution (MaHA + PBS + RGD peptide) was sterilized under UV light for 10 minutes prior to adding biomolecules and was crosslinked in a Teflon mold 8 mm in diameter and 1 mm in height (~ 70 μL) for 30 minutes. Six weeks after implantation, the rats were euthanized using CO_2 asphyxiation and the crania were harvested and fixed in 4% phosphate-buffered formalin. All animal procedures were approved by the University of Pennsylvania's Institute for Animal Care and Use Committee (IACUC).

New bone formation within the treated defects was quantified using both planar radiography (Faxitron cabinet system, model #43855A, 25 kV, 15 s) and micro-computed tomography (μCT, Scanco Medical VivaCT 75 μCT scanner with X-Ray acquisition settings at 70 kVp and 114 μA, a 20.5 μm isotropic voxel size, and an integration time of 381 ms) and compared to the negative control (empty defect). For planar radiography, the percent radiopacity in each defect was quantified using ImageJ software. For μCT, Scanco computer software was used to create three-dimensional reconstructions of the scanned tissue with bone volume in the defects quantified using a consistent threshold value of μ=1.26/cm (software value of 158) for all samples. Using a top view of the three-dimensional reconstructed tissue, each sample also received a score to represent the degree of bone bridging across the defect (see Supplementary Information for scoring details).[24]

After imaging, tissue samples were decalcified in 10% ethylenediaminetetraacetic acid (EDTA; Sigma-Aldrich) for three weeks, dehydrated, embedded in paraffin (Polysciences), and sectioned into 10 μm sections. Paraffin-embedded tissue sections were stained with

hematoxylin and eosin (H&E; Sigma-Aldrich) according to standard techniques. Individual images were stitched together using the MosaicJ stitching plug-in available for ImageJ.[28]

Statistics

All values are reported as mean ± standard deviation for at least three independent samples. Where indicated, statistical analysis was performed using a one-way analysis of variance (ANOVA) followed by a Tukey's post hoc test with a 95% confidence interval.

Supplementary Material

Refer to Web version on PubMed Central for supplementary material.

Acknowledgements

The authors would like to acknowledge the National Institute of Arthritis and Musculoskeletal and Skin Diseases (NIAMS), part of the National Institutes of Health (NIH), for funding under Award Number F32AR063598. Additional funding was provided by the Department of Defense under Grant Number OR090203. The authors would also like to acknowledge the research division within Philadelphia's Veterans Affairs Medical Center for use of their μCT.

References

1. Carragee EJ, Hurwitz EL, Weiner BK. Spine J. 2011; 11:471. [PubMed: 21729796]
2. Kitaori T, Ito H, Schwarz EM, Tsutsumi R, Yoshitomi H, Oishi S, Nakano M, Fujii N, Nagasawa T, Nakamura T. Arthritis Rheum. 2009; 60:813. [PubMed: 19248097]
3. Lau TT, Wang D-A. Expert Opin. Biol. Ther. 2011; 11:189. [PubMed: 21219236]
4. O'Keefe RJ, Mao J. Tissue Eng. Part B. 2011; 17:389.
5. Silber JS, Anderson DG, Daffner SD, Brislin BT, Leland JM, Hilibrand AS, Vaccaro AR, Albert TJ. Spine. 2003; 28:134. [PubMed: 12544929]
6. Shrivats, AR.; Alvarez, P.; L Schutte, JO. Hollinger. In: Lanza, R.; Langer, R.; Vacanti, JP., editors. Principles of Tissue Engineering. Fourth Edition. Elsevier; London, UK: 2014. p. 1201-1221.
7. Bessa PC, Casal M, Reis RL. J. Tissue Eng. Regen. Med. 2008; 2:81. [PubMed: 18383454]
8. White AP, Vaccaro AR, Hall JA, Whang PG, Friel BC, McKee MD. Int. Orthop. 2007; 31:735. [PubMed: 17962946]
9. Hsu WK, Wang JC. Spine J. 2008; 8:419. [PubMed: 18375186]
10. Geiger M, Li RH, Friess W. Adv. Drug Delivery Rev. 2003; 55:1613.
11. Yu L, Cecil J, Peng S-B, Schrementi J, Kovacevic S, Paul D, Su EW, Wang J. Gene. 2006; 374:174. [PubMed: 16626895]
12. Yagi H, Soto-Gutierrez A, Parekkadan B, Kitagawa Y, Tompkins RG, Kobayashi N, Yarmush ML. Cell Transplant. 2010; 19:667. [PubMed: 20525442]
13. Hosogane N, Huang Z, Rawlins BA, Liu X, Boachie-Adjei O, Boskey AL, Zhu W. Int.
14. Ji W, Yang F, Ma J, Bouma MJ, Boerman OC, Chen Z, van den Beucken JJJP, Jansen JA. Biomaterials. 2013; 34:735. [PubMed: 23117215]
15. Herberg S, Susin C, Pelaez M, Howie RN, Moreno de Freitas R, Lee J, Cray JJ, Johnson MH, Elsalanty ME, Hamrick MW, Isales CM, Wikesjö UME, Hill WD. Tissue Eng. Part A. 2014
16. Lutolf MP, Lauer-Fields JL, Schmoekel HG, Metters AT, Weber FE, Fields GB, Hubbell JA. Proc. Natl. Acad. Sci. U.S.A. 2003; 100:5413. [PubMed: 12686696]
17. Zisch AH, Lutolf MP, Ehrbar M, Raeber GP, Rizzi SC, Davies N, Schmökel H, Bezuidenhout D, Djonov V, Zilla P, Hubbell JA. FASEB J. 2003; 17:2260. [PubMed: 14563693]
18. Holloway JL, Ma H, Rai R, Burdick JA. J. Controlled Release. 2014
19. Burdick JA, Prestwich GD. Adv. Mater. 2011; 23:H41. [PubMed: 21394792]

20. Yoo HS, Lee EA, Yoon JJ, Park TG. Biomaterials. 2005; 26:1925. [PubMed: 15576166]
21. Huang L, Cheng YY, Koo PL, Lee KM, Qin L, Cheng JCY, Kumta SM. J. Biomed. Mater. Res. Part A. 2003; 66:880.
22. Purcell BP, Elser JA, Mu A, Margulies KB, Burdick JA. Biomaterials. 2012; 33:7849. [PubMed: 22835643]
23. Hamidi M, Azadi A, Rafiei P. Adv. Drug Delivery Rev. 2008; 60:1638.
24. Spicer PP, Kretlow JD, Young S, Jansen JA, Kasper FK, Mikos AG. Nat. Protoc. 2012; 7:1918. [PubMed: 23018195]
25. Khetan S, Guvendiren M, Legant WR, Cohen DM, Chen CS, Burdick JA. Nat. Mater. 2013; 12:458. [PubMed: 23524375]
26. Sahoo S, Chung C, Khetan S, Burdick JA. Biomacromolecules. 2008; 9:1088. [PubMed: 18324776]
27. Khetan S, Katz J, Burdick JA. Soft Matter. 2009; 5:1601.
28. Thévenaz P, Unser M. Microsc. Res. Tech. 2007; 70:135. [PubMed: 17133410]

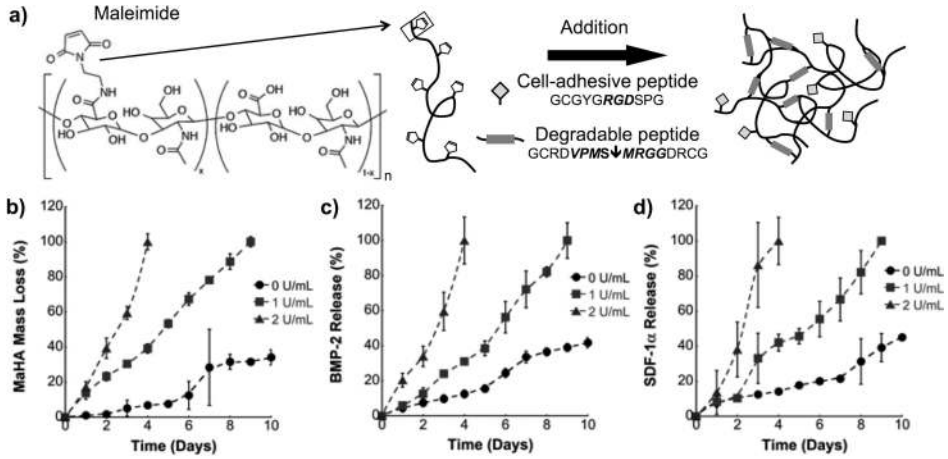

Figure 1.

(a) Schematic showing MaHA hydrogel formation: MaHA was combined with both cell-adhesive peptides (RGD, pendent) and MMP-sensitive peptides (VPMS↓MRGG, crosslinker), where an addition reaction occurred rapidly between the maleimide functional groups on HA and the thiols within the cysteine residues on the peptides. Hydrogels were loaded with both SDF-1α and BMP-2 in which (b) hydrogel mass loss, (c) BMP-2 release, and (d) SDF-1α release were measured as a function of time in 0, 1, and 2 U/mL collagenase. Error bars represent standard deviations from the mean (n = 4).

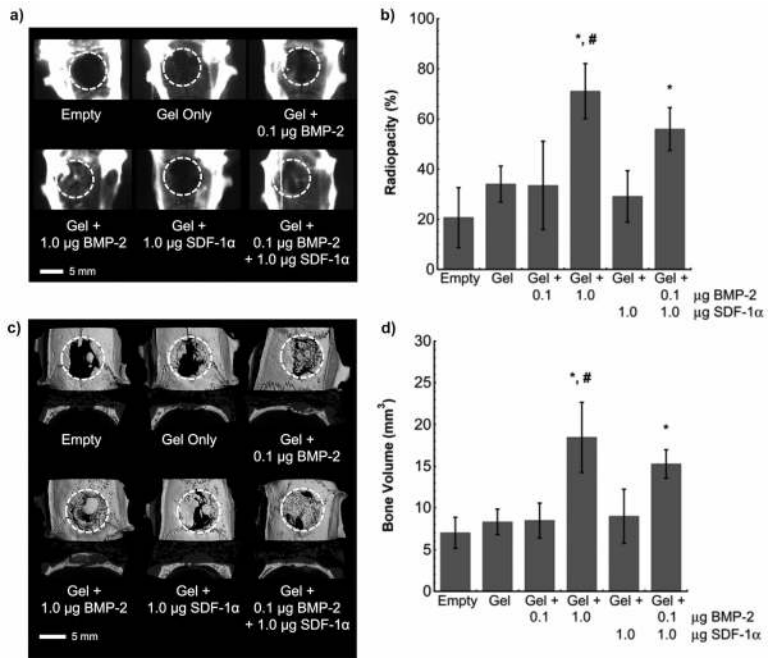

Figure 2.

(a) Representative radiographs and (b) their quantification, as well as (c) three-dimensional μCT reconstructions (top view and cross-section) with dashed circles indicating approximate calvarial defect area and (d) their quantification six weeks after treatment. Statistical significance ($p < 0.05$): (*) compared to empty defect and (#) compared to the hydrogel without biomolecules. Error bars represent standard deviations from the mean (n = 3).

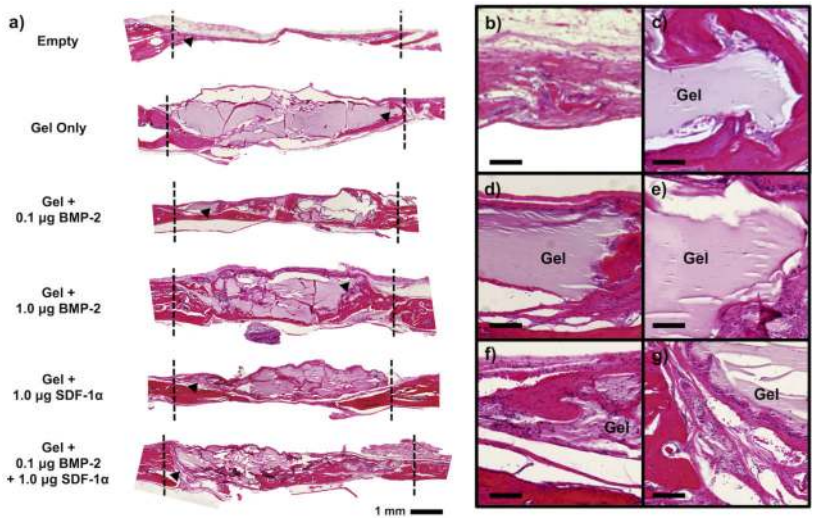

Figure 3.

(a) Representative hematoxylin and eosin (H&E) stained calvarial defects for all treatment groups at six weeks, where the approximate defect boundaries are indicated with dashed lines. Higher magnification images (at the black arrowheads) showing the boundary area between the bone and hydrogel material for the (b) empty defect, (c) hydrogel alone, (d) hydrogel with 0.1 μg BMP-2, (e) hydrogel with 1.0 μg BMP-2, (f) hydrogel with 1.0 μg SDF-1α, and (g) hydrogel with both 0.1 μg BMP-2 and 1.0 μg SDF-1α. Scale bar for higher magnification images is 0.1 mm.